Professor Stan Kolaczkowski 10 Dec 2015

Department of Chemical Engineering

University of Bath, Bath, UK

Steam gasification of a refuse derived char: Reactivity and kinetics

C. D. Le [a, b,*], S. T. Kolaczkowski [b]

[a] Department of Oil Refining and Petrochemistry, Hanoi University of Mining and Geology, Duc Thang, Bac Tu Liem, Hanoi, Vietnam

[b] Department of Chemical Engineering, University of Bath, Bath, BA2 7AY, UK

Abstract

A char was obtained from a commercial pilot-scale gasifier, which had been operating with a refuse derived fuel (RDF). Using this char, steam gasification experiments were then performed in a 15.6 mm i.d. packed bed tubular reactor. The effect of reaction temperature was studied (800 ºC to 900 ºC), and also the partial pressure of steam were in the range 33.3 kPa to 66.7 kPa. With the aid of the Shrinking-Core and the Uniform-Reaction models, kinetic parameters were estimated (apparent activation energy varied from 96 kJ mol^{-1} to 162 kJ mol^{-1}). It was also found that at lower carbon conversions (e.g. 10 % to 60 %) the RDF-derived char appeared to be more reactive than other bio-chars reported in the literature. However, at higher conversions (> 60 %), its apparent reactivity decreased with carbon conversion, thereby behaving in a similar manner to chars derived from coal.

Key words: Kinetic, steam gasification, RDF-derived char, biomass.

[*] Corresponding author: Tel: +44 1225 384543. Fax: +44 1225 385713. *E-mail addresses:* C. D. Le (ledinhchien@humg.edu.vn, chien.dinh.le@bath.edu); S. T. Kolaczkowski (s.t.kolaczkowski@bath.ac.uk);

1. Introduction

There is much interest in the development of processes in which biomass (e.g. wood) and refuse derived fuels (RDFs) may be converted into a gaseous stream, which could then be used as a fuel to produce energy, or act as a chemical intermediate. Based on information in the literature, it is well recognized that when biomass is gasified in the presence of air, then a gas mixture of CO, H_2, CO_2, N_2 and H_2O is produced, and a char stream is also produced as a by-product [1, 2, 3, 4]. In such processes, the char arises from the nature of the gasification process, where some of the carbon in the feedstock remains, combined with the residual ash, which needs to be removed from the process. As such biomass gasification processes are being developed, there has been great interest in the conversion of the residual carbon in the char into a gaseous fuel, and such a process could be developed using steam to gasify the char.

1.1. Motivation for the gasification of RDF derived char

In their discussions with a number of different companies that were developing such biomass to energy processes, the authors of this paper were made aware of the importance that such companies placed on the need to find economically viable ways of

List of Abbreviations

AAEM	Alkali and Alkaline Earth Metallic
QMS	Quadrupole Mass Spectrometer
RDF	Refuse Derived Fuel
TGA	Thermo Gravimetric Apparatus

converting the carbon in the char into a useful form of gaseous fuel. Otherwise, the char produced had to be disposed of off-site, which created a disposal cost and a loss in revenue from the potential of converting the carbon in the char into gaseous fuel. These considerations led to the work described in this study. In such processes, there is thermal energy available, which could be used to produce steam on-site. So using steam in such a process makes sense.

Although there have been many kinetic studies performed on the steam gasification of char [5, 6, 7], these in general have been performed on char from wood, food waste, and coal. There is relatively little data on the gasification of char produced from a process using a refuse derived fuel (RDF). However, it is well recognized that char reactivity depends not only on operating parameters (e.g. temperature, pressure, steam ratio), but also on the source of the char and how it was produced. For example, wood char reactivity is reported to increase with carbon conversion [8], whereas that of coal char decreases with carbon conversion [9]. The presence of inorganic elements in the char may also have a favourable catalytic effect, e.g. [1]

1.2. Effect of temperature

Many of the studies in the literature on the steam gasification kinetics of chars are performed at temperatures in the region of 700 ºC to 1000 ºC, reflecting the temperature range inside the reaction zone of a gasifier (fluidized/fixed bed), for example, in:

Paviet *et al*. [10] - char gasification experiments are performed with steam at 850 ºC, 900 ºC, 950 ºC and 1000 ºC.

Khor *et al*. [11] - charcoal gasification experiments are performed with steam and air at 800 ºC to 950 ºC in the bed.

Chaudhari *et al*. [3] - steam gasification of chars at 700 ºC, 750 ºC, and 800 ºC. According to Blasi [12], at such high temperatures (<1000 ºC), the rate of diffusion through the pores of reacting chars plays no role in determining the overall rate of reaction, so measurements at such high temperatures are considered to be in the kinetically controlled regime. In some of the studies reported in the literature, by making comparisons between the time-scales of the different phenomena involved, a simplified approach to kinetic analysis has been adopted. Such a technique is described in Dupont *et al*. [13], who applied it to a study on the gasification of biomass with steam.

Particle size will also have an effect, and this is discussed in Section 1.4.

1.3. Effect of gas velocity

The effect of gas velocity was also considered in some studies. For example, Paviet *et al*. [5] reported that gas velocity had influence on the external mass transfer resistance, and at high gas velocity (from 10 cm s^{-1} to 20 cm s^{-1}) this influence could be considered to be negligible. Mermoud *et al*. [8] also suggested that gas velocity had a gentle influence on gasification.

1.4. Effect of particle size

Char particle size was reported to have no effect by some authors (e.g. Paviet *et al*. [5]), while others (e.g. Mermoud *et al*. [8]; Mani *et al*. [14]) have reported that as the particle size is increased, then this has a retarding effect on the rate.

Paviet *et al*. [5], in an investigation of the effects of diffusional resistance on wood char gasification in a tubular kiln reactor, reported no significant influence on wood char gasification for mean char particle sizes of 0.1 mm and 0.47 mm. They suggested that internal mass transfer effects at these conditions could be considered to be negligible (experiments at T = 900 ºC to 1000 ºC, and steam partial pressure from 10.1 kPa to 70.9 kPa).

Mani *et al*. [13], in an investigation of reaction kinetics and mass transfer of wheat straw char with CO_2 using a thermo gravimetric apparatus (TGA), found that particle size (from less than 60 μm to 925 μm) had much influence on the char gasification reaction, and reactivity decreased as the particle size increased (experiments performed at T = 750 ºC to 900 ºC, with CO_2 partial pressure of 101 kPa).

Mermoud *et al*. [8] formed similar conclusions as Mani *et al*. [14]. However, they investigated the steam gasification of single wood charcoal particles (10 mm to 30 mm in size) at different temperatures (830 ºC to 1030 ºC), and at different steam partial pressures (10.1 kPa to 40.5 kPa). They concluded that internal mass transfer was influencing the reaction under these operating conditions – although this is not surprising as the charcoal particles were relatively large.

1.5. Effect of alkali and alkaline metallic (AAEM) species

113 It is well-known that AAEM species can act as good catalysts for the
114 combustion and gasification of solid carbonaceous fuels such as biomass or biochar [1,
115 15]. As reported in Yip *et al*. [15], during char gasification, the reactivity of the raw
116 biochars generally increased, while that of all acid-treated biochars (for removal of
117 AAEM species) remained relatively unchanged with conversion. The results indicate
118 that Na, K, and Ca retained in the biochars were the key catalytic species, with the
119 catalytic effect appearing to be in the order K > Na > Ca during the steam gasification
120 of the biochar.
121 A similar phenomenon of increased reactivity of biochar with conversion was
122 also observed and reported by Wu *et al*. [1]. The catalytic effect of the inherent AAEM
123 species seems in turn to depend on the carbon structure that probably affects the catalyst
124 dispersion. It was emphasized that the surface area of biochar increased with
125 conversion, suggesting the formation of new pores and/or opening of closed pores as a
126 result of steam activation during gasification. Besides the effect of the carbon structure
127 evolution, the inhibiting effect of some inorganic components such as Si and P was also
128 discovered by Hugnon et al. [16], where K would tend to be encapsulated by P and Si
129 with carbon conversion, and would then be unable to act as a catalyst.
130 Nevertheless, consideration of the effects of catalysts and evolution of carbon
131 structure during gasification will not be considered in any detail in this paper; however,
132 they will be used to explain the evolution of reactivity of RDF-derived char during the
133 gasification process.
134
135 ***1.6. Decisions taken***
136

Based on this review, it was decided that the influence of: char particle size, gas flow, char bed length, reaction temperature and steam partial pressure should all be explored. This would lead to the development of useful kinetic rate expressions, which in the future could be used to help estimate the residence time required in a reactor to achieve the desired conversion of carbon in the char. This work is clearly novel, as there is relatively little information in the literature on the gasification kinetics of RDF-derived char.

In developing the experimental technique, a number of important assumptions were made based on the following:

(a) In the literature, it has been suggested (e.g. Everson *et al*. [17] and Huang *et al*. [18]) that char-CO_2 and char-H_2O reactions proceed on separate active sites at atmospheric pressure. Thus, in this present study, it was decided to study the steam (H_2O) gasification of char as a set of experiments on their own.

(b) Although some authors (e.g. Everson *et al*. [17]; Huang *et al*. [18]) have presented evidence of the inhibition effects of CO in CO_2-char reactions, and H_2 in steam-char reactions, in this study it is assumed that there are no inhibition effects.

(c) The partial pressure of the gasifying agent (H_2O) is considered to remain unchanged along the reactor, even though it is inevitably consumed in reality. This assumption was also applied in other studies in the literature (e.g. Wu *et al*. [7]; Yip *et al*. [15]).

(d) Many of the kinetic experiments on char gasification have been performed using a TGA, and the carbon conversion was measured by the loss in the weight of the sample [8, 14, 17, 18, 19]. However, in this study, it was decided to perform

such experiments in a small packed-bed reactor, which is often used in heterogeneous catalytic experiments. A fast gas analysis method developed in [20] using a quadrupole mass spectrometer (QMS) was used to measure the product gas composition on-line, which was then used to calculate the rate of carbon conversion in the char.

2. Experimental Procedure

2.1. Experimental Apparatus

The experimental work was carried out using a packed-bed reactor (Figure 1), which operated at atmospheric pressure. The reactor consisted of a vertical stainless steel tube with an inner diameter of 15.6 mm, which was filled with RDF-derived char particles. The char bed depth could be varied from 1.6 mm to 23.7 mm. This tube was positioned inside an electrically heated furnace, and the temperature inside the char bed was measured using a thermocouple located at the top of the char bed. The char bed was supported by two quartz wool layers which retained the char and ash particles.
In experiments with steam, the water and nitrogen passed through a stainless steel tube put inside the furnace, which vaporized the water and preheated the gas. The nitrogen flow was adjusted with a rotameter, while that of the water was set using a metering pump.

The gas exiting from the top of the reactor flowed through a cooling coil, and condensate was trapped in two plastic vessels (connected in series). The gas then passed through a glass wool filter, and was finally discharged into the vent from the fume

cupboard. A gas sample stream was passed to a quadrupole mass spectrometer (QMS) for on-line gas analysis.

Figure 1 here

2.2. RDF-derived Char Particle Size Distribution

Sieves were used to classify by size the RDF-derived char that had been obtained from the commercial pilot-scale gasifier. Information on the fixed carbon content in the different char size ranges will be also useful when designing a process.

The frequency mass fractions were calculated from:

$$q_i = \left(\frac{m}{\Delta d_q} \right)_i \quad \text{or} \quad \mathrm{Q_i} = \sum_1^i \left(q \Delta d_q \right)_i \tag{1}$$

where: q_i is the differential frequency mass (or fixed carbon content) fraction of size interval i , μm^{-1}; Q_i is the cumulative frequency mass (or fixed carbon content) fraction of particles smaller than size $(d_q)_i$; $(\Delta d_q)_i$ is the size interval i, μm; and m_i is the mass fraction of char particle in size interval i.

Then, the mean size of the RDF-derived char particles was estimated from:

$$\bar{d}_q = \frac{1}{\sum^{all\ i} \left(m / d_q \right)_i} = 305.52\ \mu m \tag{2}$$

The results of such a char particle distribution are presented, in Figure 2, from which it can be seen that particle size varied from 37.5 μm to 7,000 μm. As the mean size of the RDF-derived char was 305 μm, a sieve was used to obtain a char particle size range of 250 to 500 μm (representing mean particle size), and this size range was used for the experiments.

208

209 ***Figure 2 here***

210

211 From the data on the fixed carbon content (Figure 2(c)), it is interesting to note
212 that this changes slightly with particle size, and this is most probably related to the part
213 of the process from which that carbon particle arose (e.g. carried in the gas stream and
214 trapped in a cyclone, or retained in the char stream from the base of the gasifier).
215 The results of proximate analysis of the RDF-derived char are: moisture 4.59
216 wt.% wet basis; volatiles 10.71 wt.% dry basis; fixed carbon 34.18 wt.% dry basis; ash
217 55.10 wt.% dry basis. The proximate analysis of the RDF pellets was also performed,
218 giving: moisture 7 wt.% wet basis; volatiles 43 wt.% dry basis; fixed carbon 31 wt.%
219 dry basis; ash 26 wt.% dry basis.
220 From these measurements, it was decided to use char in the size range of 250
221 μm to 500 μm for the kinetic experiments.

222

223 **2.3. Experimental Methodology**

224

225 A bucket of RDF-derived char, obtained from an actual gasification pilot-plant
226 that used RDF pellets as fuel, was supplied by Refgas Ltd, Sandycroft. This char was
227 sealed and stored at room temperature, and used throughout this study to ensure the
228 repeatability of the char resource.
229 Samples of char were first conditioned by heating for 3 hours in a flow of N_2 at
230 800 ^{o}C, and this removed any volatiles (checked with the QMS). Then N_2 was fed into
231 the reactor (during the heating-up period) to achieve the desired operating temperature.

232 This was then followed by the addition of water which turned into steam, and the
233 experiment was started. The system pressure was atmospheric (open end of reactor).
234 After each run, air was passed through the reactor to burn out any residual carbon.
235 Finally, the reactor was cooled, and the remaining ash was collected and weighed.

236 The rate of carbon conversion in the char can be inferred from the molar flow
237 rate of CO and CO_2 from the reactor. This approach has been used in many studies [5, 6,
238 7, 9, 10], making use of the flow of an inert sweeping gas (e.g. N_2 or Argon) to perform
239 such calculations. If the formation of CH_4 was significant then it would have to be
240 included, but this was checked and found not to be the case in the experiments
241 described.

242 The experimental conversion of carbon in the char, *X*, may be defined (e.g. in
243 Paviet *et al*.[5]) as:

244 $$X = \frac{w_0 - w}{w_0 - w_{ash}} \tag{3}$$

245 where: w_0 is the initial sample weight, w is the sample weight at any time t and w_{ash} is
246 the ash content measured after reaction.

247 The evolution of sample weight, *w(t),* as a function of time is unknown, but it
248 can be deduced from the gas composition. The experimental kinetic rate, at any time *t*,
249 can thus be calculated (e.g. in Cozzani [19]) from:

250 $$\frac{dX}{dt} = \lim_{\Delta t \to 0}\left(\frac{X_{t_2} - X_{t_1}}{\Delta t}\right) \tag{4a}$$

251 where: X_{t_1} and X_{t_2} are carbon conversion at time t_1 and t_2, respectively; and

252 $\Delta t = t_2 - t_1 \approx 20\ s$, which is the measurement step of the gas analysis method.

253 or (e.g. in Paviet *et al*. [5]) from:

$$\frac{dX}{dt} = \frac{12\left(F_{CO} + F_{CO_2}\right)}{w_0 - w_{ash}} \quad (4b)$$

where: F_{CO} and F_{CO_2} are molar flow rates (mol/min) of CO and CO_2, respectively, in the gas stream from the packed bed.

Both Equations (4a) and (4b) were tested, and they produced the same results. Equation (4b) was used in this work.

3. Results and Discussion

3.1. Experimental Results

To determine the operating conditions for the kinetic study the following set of preliminary experiments was performed:

3.1.1. Effect of char bed length

First of all, some preliminary experiments were performed with different char bed lengths (1.6 mm, 5.7 mm, 8.2 mm,16.8 mm and 23.7 mm), corresponding to different initial mass quantities of char (0.1 g, 0.35 g, 0.5 g, 1.03 g and 1.45 g). The bulk density of the char is 500 kg m^{-3}. Experiments were performed at: furnace temperature set at 900 ^oC; char particles from 250 μm to 500 μm; N_2 flow set at 0.2 L min^{-1} (1 L = 1 dm^3; 1 min = 60 s); H_2O flow set at 0.148 g min^{-1}; and an calculated molar ratio of H_2O:N_2 = 1:1.

It was observed that the performance of the reactor with bed lengths from 1.6 mm to 16.8 mm was very similar and about 70 % of the carbon in the char was

consumed after eight minutes. This means that in such a sample the resistance to external mass transfer is negligible.

For the planned kinetics study, it was decided to select a small initial bed length to reduce any secondary reactions, and to minimize the change in the partial pressure of steam along the char bed. However, if a bed length < 5.7 mm was used, then CO concentration would be low, leading to measurement errors. Therefore, an initial char bed length of 8.2 mm was selected for all subsequent experiments.

3.1.2. Effect of gas flow

Experiments were performed at different gas inlet flows (N_2 = 0.2 L min^{-1}, 0.4 L min^{-1}, 0.6 L min^{-1} and 0.7 L min^{-1}; H_2O = 0.148 g min^{-1}, 0.296 g min^{-1}, 0.444 g min^{-1} and 0.518 g min^{-1}), which corresponded to different superficial velocities in the packed bed (0.218 m s^{-1}, 0.437 m s^{-1}, 0.655 m s^{-1} and 0.764 m s^{-1}). The experiments were done at the following conditions: furnace temperature set at 900 °C; char bed length = 8.2 mm; char particles from 250 μm to 500 μm; calculated molar ratio of H_2O:N_2 = 1:1.

It was observed that at the high gas superficial velocities (0.437 m s^{-1} to 0.764 m s^{-1}), the gas velocity has little influence on char gasification, indicating that external mass transfer resistance is low. In Paviet *et al*. [5], superficial gas velocities at 10 cm s^{-1} to 20 cm s^{-1} (0.1 m s^{-1} to 0.2 m s^{-1}) had little influence on external mass transfer. Although high gas velocities are preferred, this leads to higher errors in CO measurements in the outlet gas stream; hence, a gas velocity of 0.218 m s^{-1} was selected for subsequent experiments.

3.1.3. Effect of char particle size

Experiments were performed with char particles that had the following size ranges: 180 μm to 250 μm; 250 μm to 500 μm; 1000 μm to 1180 μm; and 2000 μm to 4000 μm. The experiments were done at: furnace temperature set at 900 °C; char bed length = 8.2 mm; N_2 flow set at 0.2 L min^{-1}; H_2O flow set at 0.148 g min^{-1}; calculated molar ratio of H_2O:N_2 = 1:1.

The results obtained showed that the rate of carbon conversion increases slightly as the particle size was reduced. However, the increase was insignificant in the size range tested. Also, because the measured mean particle size of RDF-derived char was approximately 305 μm, particles in the range of 250 μm to 500 μm were chosen for the subsequent kinetic experiments.

3.1.4. Effect of Reaction Temperature

To explore the effect of reaction temperature, experiments were performed at: 800 °C, 850 °C and 900 °C. This set of experiments (at different reaction temperature) was repeated at various H_2O flows, while N_2 flow was kept constant at 0.2 L min^{-1}. This helps to determine kinetic parameters that will be described later. One example of the conditions in the reactor for one set of experiments was: N_2 flow rate = 0.2 L min^{-1}; char bed length = 8.2 mm; H_2O flow = 0.222 g min^{-1}; calculated molar ratio of H_2O:N_2 = 3:2, corresponding to steam partial pressure of 60 kPa.

As expected, reaction rates increased with temperature, see Figure 3.

Figure 3 here

3.1.5. Effect of Partial Pressure of Steam

As a reminder, for each reaction temperature (800 ºC, 850 ºC, or 900 ºC), experiments were performed at different partial pressures of H_2O (33.3 kPa, 50 kPa, 60 kPa and 66.7 kPa), which corresponded to different H_2O flows (0.074 g min^{-1}, 0.148 g min^{-1}, 0.222 g min^{-1} and 0.296 g min^{-1}), while N_2 flow was kept constant at 0.2 L min^{-1}. One example of the conditions in the reactor was: furnace temperature set = 850 ºC; N_2 flow = 0.2 L min^{-1}; char bed length = 8.2 mm.

The results are presented in Figure 4, for experiments performed at 850 ºC. From these experiments, char reactivity increases with steam partial pressure.

Figure 4 here

3.2. Kinetic Analysis

There are several well established approaches which can be used to develop a model to describe reacting char. Because the ash content in the RDF-derived char is high, then according to Levenspiel [21] and Kunii and Levenspiel [22], then either the Uniform-Reaction Model or the Shrinking-Core Model for porous solids of unchanging size could be applied. In general, small particles follow the Uniform-Reaction Model, while large particles follow the Shrinking-Core Model - with ash diffusion controlling at high temperatures, but reaction controlling at low temperatures [22]. In this study, both of these models were considered.

3.2.1. Estimate of Kinetic Parameters for the Shrinking-Core Model

347 The theoretical development of this model is based on Levenspiel [21] and
348 Kunni and Levenspiel [22]. In summary: for a Shrinking-Core model, the reaction front
349 advances from the outer surface into the particle, leaving behind a layer of ash. Thus, at
350 any time there exists an unreacted core of carbon which shrinks in size during the
351 reaction. The driving force of the gasification is proportional to the available surface
352 area, and char reactivity of a batch particle can be defined as:

353 $$r = \frac{1}{(1-X)^{2/3}} \frac{dX}{dt} = k.P_{H_2O}^{n} \quad (5)$$

354 where: $r = \frac{1}{(1-X)^{2/3}} \frac{dX}{dt}$ is called specific (or apparent) reactivity of char in
355 gasification reaction [15].

356 A similar equation to Equation (5) can also be seen in the literature (e.g.
357 Liliedahl and Sjostrom [23]; Basu [24]).

358 For the steam gasification of char, an n^{th}-order reaction model is commonly used
359 [6, 24]:

360 $$r = k.P_{H_2O}^{n} \quad (6)$$

361 where: P_{H_2O} is the partial pressure of steam, that is considered as the partial pressure of
362 steam in the inlet gas stream.

363 From the experimental data of carbon conversion rate, the values of the rate
364 constant *k*, the reaction order *n*, apparent activation energy *E* and pre-exponential factor
365 *A* were calculated. Figure 5 shows an example of the plots to determine the values of *k*
366 and *n* at 850 ºC, and *E and A* at different degrees of conversion (*X*). These results are
367 very encouraging as the data points are positioned close to the 'best-fit' straight lines.
368 Values of *k* and *n*, *E* and *A* are shown in Tables 1 and 2, respectively. From these, the

apparent activation energy varied from 96 to 106 kJ mol^{-1} across the 10 % to 70 % conversion range, and then it increased dramatically to 152 kJ mol^{-1} at 80 % carbon conversion.

Figure 5 here

Table 1 here

Table 2 here

Blasi [12] reviewed data on the steam gasification of a number of different biochars, and reported that *E* varied from 143 to 237 kJ mol^{-1} (with a large part of the values around 180 to 200 kJ mol^{-1}), depending on reaction conditions and biochar source. This indicates that the RDF-derived char used in this study may be very active.

From data in Table 2, the value of the pre-exponential factor increases slightly with conversion across the 10 % to 70 % range, but more rapidly after that. This change may be due to the evolution of the char structure with carbon conversion. Ahmed and Gupta [6] suggested that ash might have increased the adsorption rate of steam to the char surface, leading to an increase in the pre-exponential factor. However, (a) increased porosity, and (b) access to the ash (which may have catalytic and inhibiting properties), may also have a role to play [1, 7]. The effects of carbon structure on char reactivity are also discussed in Aarna and Suuberg [25], where they concluded that the micropores (< 2 nm) probably did not participate in the gasification reaction of chars, and that the surface developed by the macropores and the mesopores (2 nm < diameter < 50 nm) was a better indicator of the reactive surface, than the total pore surface area. This conclusion is consistent with others (e.g. Paviet *et al*. [5]; Mermoud *et al*. [26])

In other studies on the steam gasification of biochars [1, 6, 8, 15, 27] pore surface area and reactivity of chars increased with conversion, while an opposite trend was observed for the steam gasification of coal chars [7, 23, 28].

It was decided, to examine the 70 % to 80 % carbon conversion region in more detail, and more data points were added. Figure 5(c) shows the Arrhenius plot for conversions from 71 % to 80 %. A 'compensation effect' is observed here, where there is a simultaneous increase in apparent activation energy and pre-exponential factor with conversion, see Table 2. This 'compensation effect' or 'isokinetic effect' has been observed and reported in the literature for char-gas reactions [6, 7], and explains the observed change that took place.

3.2.2. Estimate of kinetic parameters for the Uniform-Reaction Model

For the Uniform-Reaction Model, the driving force for the gasification is proportional to the mass of unreacted carbon in the particle, and char reactivity of a batch particle can be defined as:

$$r = \frac{1}{1-X}\frac{dX}{dt} = k.P_{H_2O}^{n} \qquad (7)$$

A similar equation to Equation (7) can also be seen in the literature [22, 23, 24].

For this model, the values of the apparent activation energies (E) and pre-exponential factors (A) at different degrees of conversion (X) are calculated and presented in Table 3.

Table 3 here

It is interesting to note, that when comparing the values of the apparent activation energy *(E)* calculated in Table 3 (Uniform-Reaction Model), with the values in Table 2 (Shrinking-Core Model), then very similar results have been obtained. This means, that the two models would produce very similar results across the range of conditions tested. However, values of the pre-exponential factor (*A*) in the Uniform-Reaction Model are different from those in the Shrinking-Core Model. Mathematically, this comes from the fact that the pre-exponential factor in Shrinking-Core Model includes the factor that is a function of the density of carbon and diameter of the char particles**,** whereas that in the Uniform-Reaction Model does not (deduced from Kunii and Levenspiel [22]).

3.3. Comparison between RDF-derived char and wood charcoal

Finally, a few experiments were performed using a wood based charcoal, obtained from a small commercial gasification reactor that used wood chips as fuel. A bucket of this char, supplied by Refgas Ltd, Sandycroft, was sealed and stored at room temperature, and used throughout this study to ensure the repeatability of this char resource. Two different ranges of wood charcoal particles were used (250 μm to 500 μm and 2000 μm to 4000 μm) and tested. All of these experiments were performed at: furnace temperature set at 900 ^{o}C; char bed length = 8.2 mm; N_2 flow set at 0.2 L min^{-1}; H_2O flow set at 0.148 g min^{-1}; calculated molar ratio of H_2O:N_2 = 1:1.

The results are shown in Figure 6.

Figure 6 here

From these data, it is clear that at low carbon conversion (< 60 %), the RDF-derived char is much more reactive than wood charcoal. However, at higher carbon conversions the opposite is true.

In some studies [15, 28], the reactivity of gasification of char is presented as the specific (or apparent) reactivity, r. If the Shrinking-Core Model is selected, then $r = \frac{1}{(1-X)^{2/3}} \frac{dX}{dt}$. Figure 6(c) shows the evolution of apparent reactivity of char with carbon conversion.

From Figure 6(c), above a carbon conversion of 60 %, the apparent RDF-derived char reactivity decreases sharply with carbon conversion. This behaviour of RDF-derived char is opposite to that of other biochars such as mallee-bimass-derived char [14] or food-waste-derived char [6]; however, it is similar to that of coal char (e.g. as presented in Wu *et al*. [7]; Liu *et al*. [9]; Liliedahl and Sjostrom [22]; Xu *et al*. [27]).

Mermoud *et al*. [8], in a study of steam gasification of single wood charcoal particles (with a diameter of 10 mm to 30 mm), observed that the reactivity of wood charcoal increased continuously with conversion due to a continuous increase in the surface area. However, Liu *et al*. [9] reported a decrease in coal char reactivity with conversion because of a decrease in the surface area.

The RDF-derived char contained 55 wt.% ash, which consisted of inorganic elements. It is well known that these elements can have a catalytic effect, which could be the main reason for the increase in reactivity at low carbon conversion (<60%). However, the presence of inorganic elements can also decrease the porosity to such an extent that the active surface area is also decreased [1, 6, 7, 12]. In addition, Hugnon et al. [16] noticed that during steam gasification of algal and lignocellulosic biomass, K

464 would tend to be encapsulated by P and Si with carbon conversion, and would then be
465 unable to act as a catalyst. Therefore, from the results obtained in this paper, at higher
466 (>60%) carbon conversion, a higher ash content is expected, which could result in an
467 encapsulation of AAEM species, a decrease in porosity (and active surface area), and
468 hence reactivity.
469
470 **4. Conclusions**
471
472 For the steam gasification of the RDF-derived char, the apparent activation
473 energy *E* varied from 96 kJ mol^{-1} to 162 kJ mol^{-1}. The reactivity of the char (at carbon
474 conversions from 10 % to 60 %) appears to be higher than other biochars reported in the
475 literature. However, at high conversions (> 60 %), the apparent reactivity of the RDF-
476 derived char decreases with carbon conversion, behaving in a similar manner to coal
477 structures.
478 Comparisons between the use of the Shrinking-Core Model and the Uniform-
479 Reaction Model produced almost identical results.
480 Information has been presented in this paper, which provides data on the
481 properties of an RDF-derived char and how it could be gasified in the presence of
482 steam. This supports the viability of converting this type of char into a useful fuel gas,
483 which would enhance the commercial viability of the overall 'RDF to energy' process.
484 Such data on RDF-derived char are scarce in the literature, and this is probably the first
485 detailed kinetic study of its type in which kinetic parameters for an RDF-derived char
486 have been determined. These parameters could be used in modelling studies to explore

different design concepts (e.g. packed-bed, moving-bed, fluidized bed) for the 'char-gasifier', although they would of course then need to be tested in pilot-scale studies.

Acknowledgment

We are grateful for the support received from Refgas Ltd a company developing biomass to energy processes, and also for the support from the Vietnam Ministry of Education & Training, in the form of a research grant for C. D. Le.

Nomenclature

A	Pre-exponential factor	$bar^{-n}\ s^{-1}$
d_q	Diameter of char particle	μm
$\overline{d}_q$	Mean char particle diameter	μm
$(\Delta d_q)_i$	Char particle size interval *i*	μm
E	Activation energy	$kJ\ mol^{-1}$
F_i	Molar flow rate of species i	mol/min
k	Specific (or apparent) reaction rate coefficient	$bar^{-n}\ s^{-1}$
m_i	Mass fraction of char particle in size interval i	
n	Reaction order	
P_{H2O}	Partial pressure of steam	bar(a)
q	Differential frequency mass (or fixed carbon content) distribution of char particle size	μm^{-1}
q_i	Differential frequency mass (or fixed carbon	

		content) fraction of size interval i	μm^{-1}
Q		Cumulative frequency mass (or fixed carbon content) distribution of char particle size	
Q_i		cumulative frequency mass fraction of particles smaller than size $(d_q)_i$	
r		Specific (or apparent) reactivity of char in gasification	s^{-1}
R_g		Universal gas constant	8.314 J.mol K^{-1}
t		Time	s
Δt		Time interval	s
T		Temperature	^oC
w		Char sample weight at any reaction time t	g
w_0		Initial char sample weight	g
w_{ash}		Ash content measured after gasification reaction of char	g
X		Carbon conversion at any reaction time t	%

References

[1] Wu H, Yip K, Tian F, Xie Z, Li CZ. Evolution of char structure during the steam gasification of biochars produced from the pyrolysis of various mallee biomass components. Ind. Eng. Chem. Res. 2009; 48(23): 10431-10438.

[2] Knoef HAM, editer. Handbook Biomass Gasification. BTG biomass technology group; 2005.

[3] Chaudhari ST, Dalai AK, Bakhshi NN. Production of Hydrogen and/or Syngas (H_2 + CO) via steam gasification of biomass-derived chars. Energy and Fuel 2003; 17(4): 1062-1067.

[4] Kolaczkowski S, Le CD, Jodlowski P. Gasification of wood pellets in an experimental quartz tube gasifier – How visual 1D experiments can aid 3D design considerations. In Proceedings of the bioten conference on biomass and biofuels 2010, Bridgwater AV, editor, CPL Press UK; 2011, p. 720-732.

[5] Paviet F, Bals O, Antonini G. The effects of diffusional resistance on wood char gasification. Process Safety and Environment Protection 2008; 86: 131-140.

[6] Ahmed II, Gupta AK. Pyrolysis and gasification of food waste: Syngas characteristics and char gasification kinetics. Applied Energy 2010; 87: 101-108.

[7] Wu S, Wu J, Li L, Wu Y, Gao J. The reactivity and kinetics of yanzhou coal chars from elevated pyrolysis temperatures during gasification in steam at 900-1200ºC. Trans IchemE, Part B, Process Safety and Environmental Protection 2006; 84(B6): 420-428.

[8] Mermoud F, Golfier F, Salvador S, Van de Steene L, Dirion JL. Experimental and numerical study of steam gasification of a single charcoal particle. Combustion and Flame 2006; 145: 59-79.

[9] Liu H, Luo C, Kato S, Uemiya S, Kaneko M, Kojima T. Kinetics of CO_2 gasification at elevated temperatures. Part I: Experimental results. Fuel Processing Technology 2006; 87: 775-781.

[10] Paviet F, Bals O, Antonini G. Kinetic study of various chars steam gasification. International Journal of Chemical Reactor Engineering 2007; 5: Article A80.

[11] Khor A, Ryu C, Yang Y, Sharifi VN, Swithanbank J. Clean Hydrogen Production via Novel Steam-Air Gasification of Biomass. WHEC 16/13-16. Lyon France; 2006.

[12] Blasi CD. Combustion and gasification rates of lignocellulosic chars. Process in Energy and Combustion Science 2009; 35: 121-140.

[13] Dupont C, Boissonnet G, Seiler JM, Gauthier P, Schweich D. Study about the kinetic processes of biomass steam gasification. Fuel 2007; 86: 32-40.

[14] Mani T, Mahinpey N, Murugan P. Reaction kinetics and mass transfer studies of biomass char gasification with CO_2. Chemical Engineering Science 2011; 66: 36-41.

[15] Yip K, Tian F, Hayashi J, Wu H. Effect of alkali and alkaline earth metallic species on biochar reactivity and syngas composition during steam gasification. Energy Fuels 2010; 24: 173-181.

[16] Hognon C, Dupont C, Grateau M, Delrue F. Comparison of steam gasification reactivity of algal and lignocellulosic biomass: Influence of inorganic elements. Bioresource Technology 2014; 164: 347-353.

[17] Everson RC, Neomagus HWJP, Kasaini H, Njapha D. Reaction kinetics of pulverized coal-chars derived from inertinite-rich coal discards: Gasification with carbon dioxide and steam. Fuel 2006; 85: 1076-1082.

[18] Huang Z, Zang J, Zhao Y, Zhang H, Yue G, Suda T, Narukawa M. Kinetic studies of char gasification by steam and CO_2 in the presence of H_2 and CO. Fuel Processing Technology 2010; 91: 843-847.

[19] Cozzani V. Reactivity in oxygen and carbon dioxide of char formed in the pyrolysis of refuse-derived fuel. Ind. Eng. Chem. Res. 2000; 39: 864-872.

[20] Le, C.D., Kolaczkowski, S. and McClymont, D.W.J. Using a quadrupole mass spectrometer for on-line gas analysis – gasification of biomass and refuse derived fuel. Fuel. 2015; 139: 337-345.

582 [21] Levenspiel O. Chemical Reaction Engineering. 3rd ed. John Wiley & Sons; 1999.
583 [22] Kunii D, Levenspiel O. Fluidization Engineering. 2nd ed. Butterworth-
584 Heinemann; 1991.
585 [23] Liliedahl T, Sjostrom K. Modeling of char-gas reaction kinetics. Fuel 1997; 76(1):
586 29-37.
587 [24] Basu P. Biomass Gasification and Pyrolysis. Elsevier Inc; 2010.
588 [25] Aarna I, Suuberg EM. Change in reactive surface area and porosity during char
589 oxidation. Twenty-Seventh Symposium (International) on Combustion/The
590 Combustion Institute ;1998, p. 2933-2939.
591 [26] Mermoud F, Salvador S, Van de Steene L, Golfier F. Influence of the pyrolysis
592 heating rate on the steam gasification rate of large wood char particles. Fuel 2006;
593 85: 1473-1482.
594 [27] Golfier F, Van de steene L, Salvador S, Mermoud F, Oltean C, Bues MA. Impact
595 of peripheral fragmentation on the steam gasification of an isolated wood charcoal
596 particle in a diffusion-controlled regime. Fuel 2009; 88: 1498–1503.
597 [28] Xu Q, Pang S, Levi T. Reaction kinetics and producer gas compositions of steam
598 gasification of coal and biomass blend chars, part 1: Experimental investigation.
599 Chemical Engineering Science 2011; 66: 2141-2148.
600

Figure Captions

Figure 1. Schematic of the kinetic study apparatus.

Figure 2. RDF-derived char particles: (a) differential frequency mass and fixed carbon content distributions, (b) cumulative frequency mass and fixed carbon content distributions, (c) fixed carbon content based on char particle size.

Figure 3. Influence of reaction temperature: (a) carbon conversion, (b) rate of carbon conversion.

Figure 4. Influence of steam partial pressure at 850 ºC: (a) carbon conversion, (b) rate of carbon conversion.

Figure 5. Plots to estimate kinetic values: (a) Example of plot to determine the values of k and n at 850 ºC (Shrinking-Core Model); (b) Arrhenius plot for conversions from 10 to 80 % (Shrinking-Core Model); (c) Arrhenius plot for conversions from 71 to 80 % (Shrinking-Core Model).

Figure 6. Comparisons between RDF-derived char and wood charcoal at 900 ºC: (a) carbon conversion, (b) rate of carbon conversion, (c) apparent reactivity.

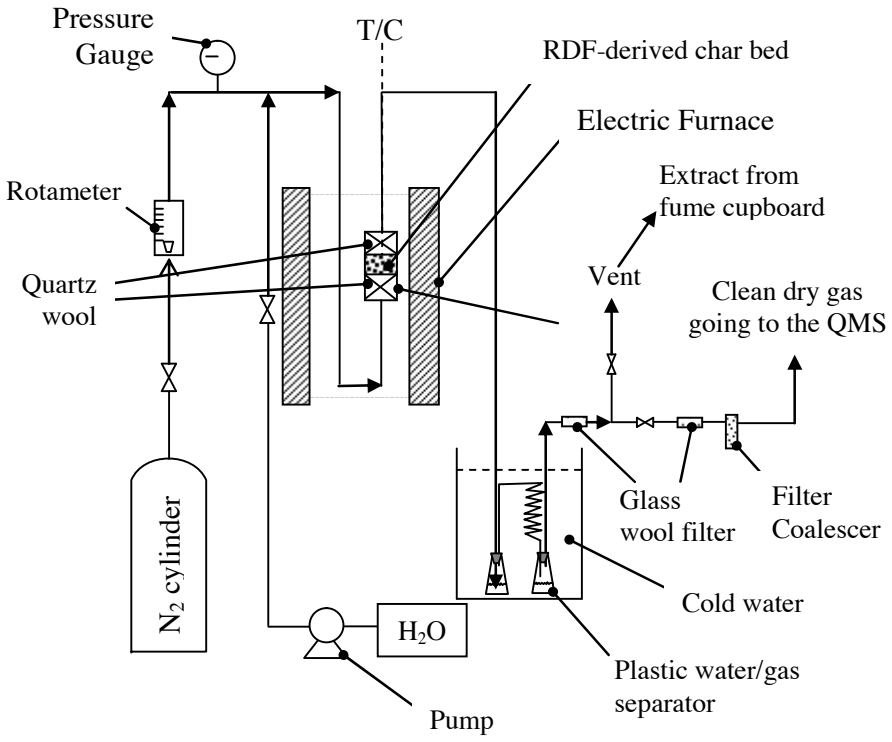

618

619 **Figure 1**

620

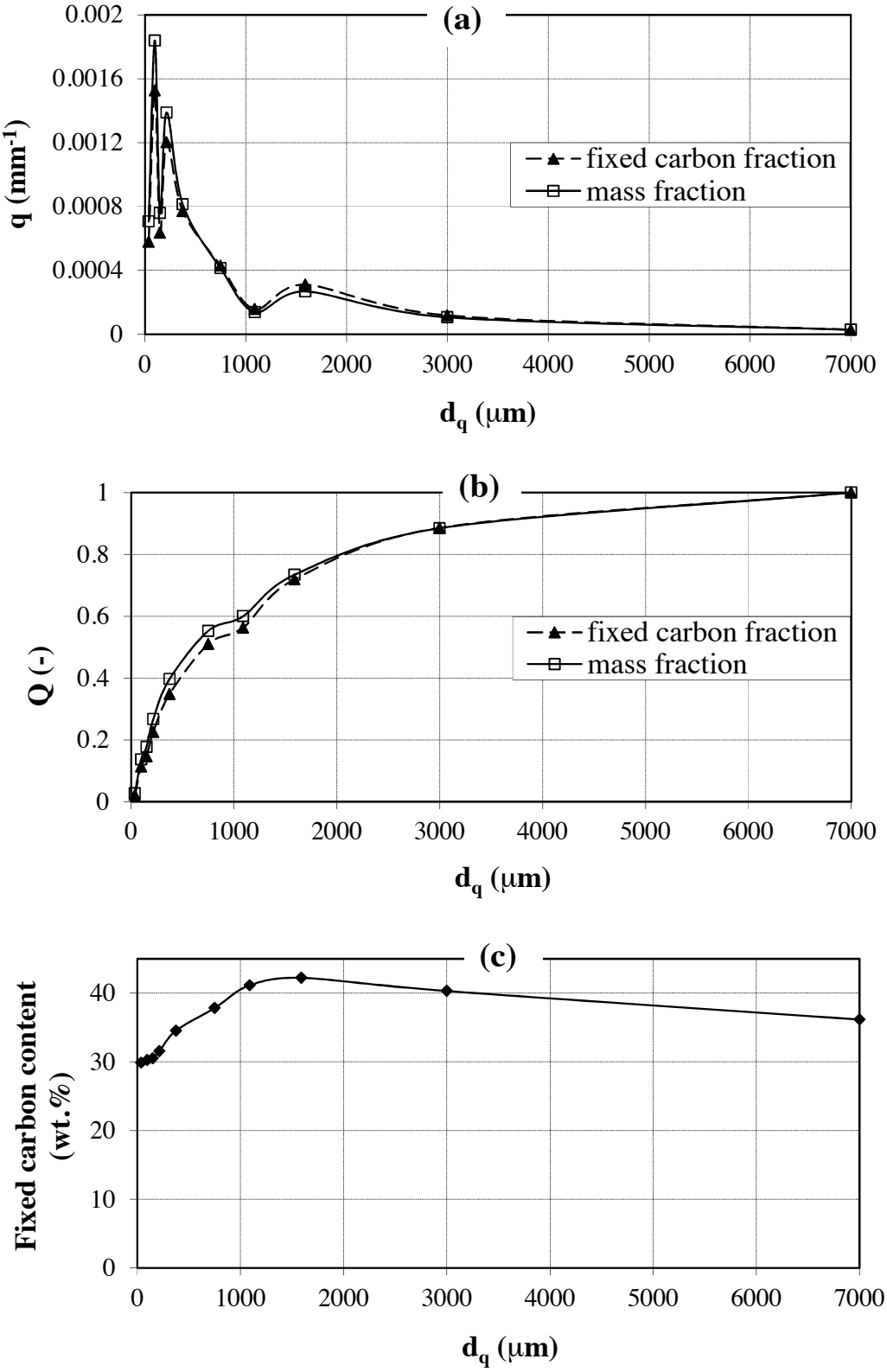

621

622 **Figure 2**

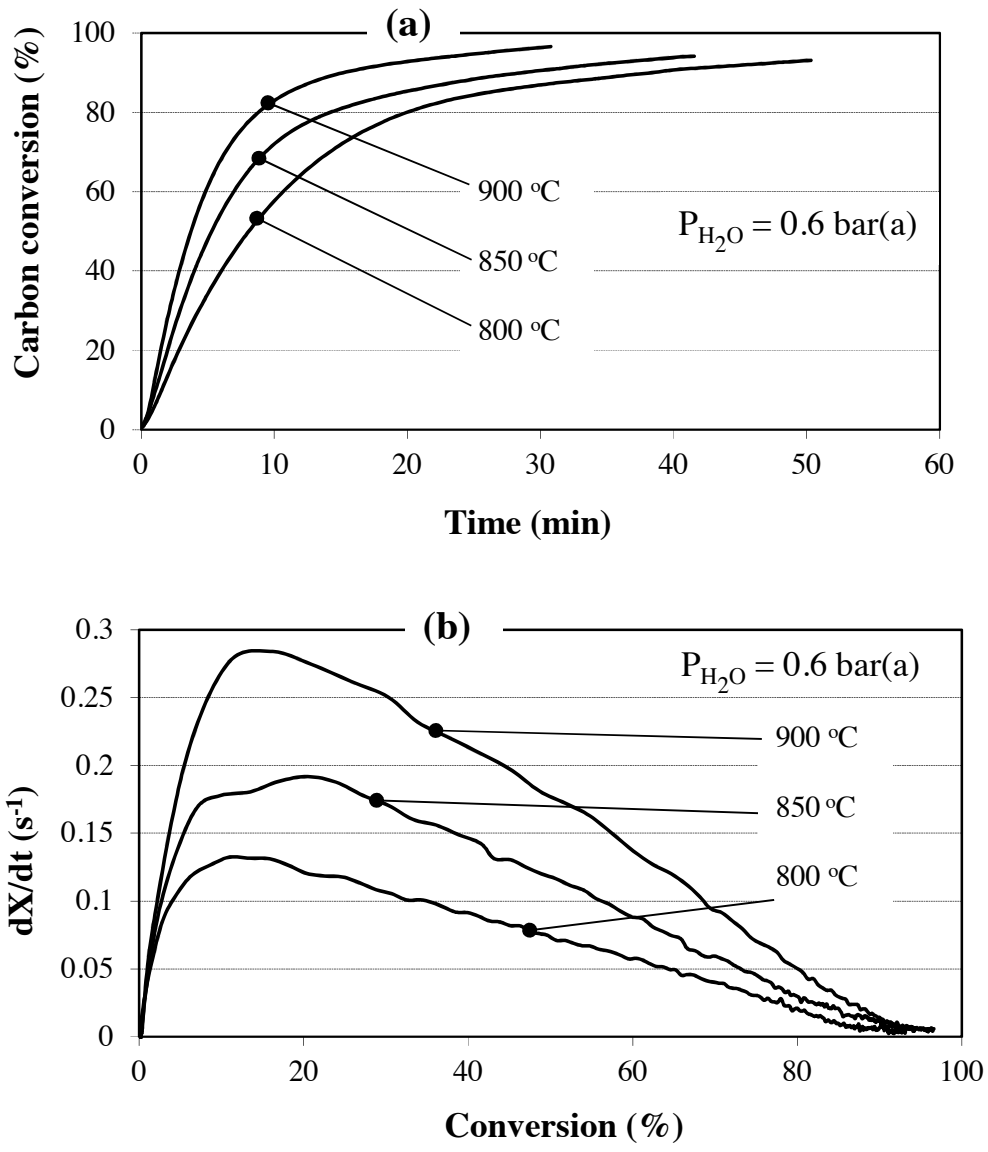

623

624 **Figure 3**

625

626

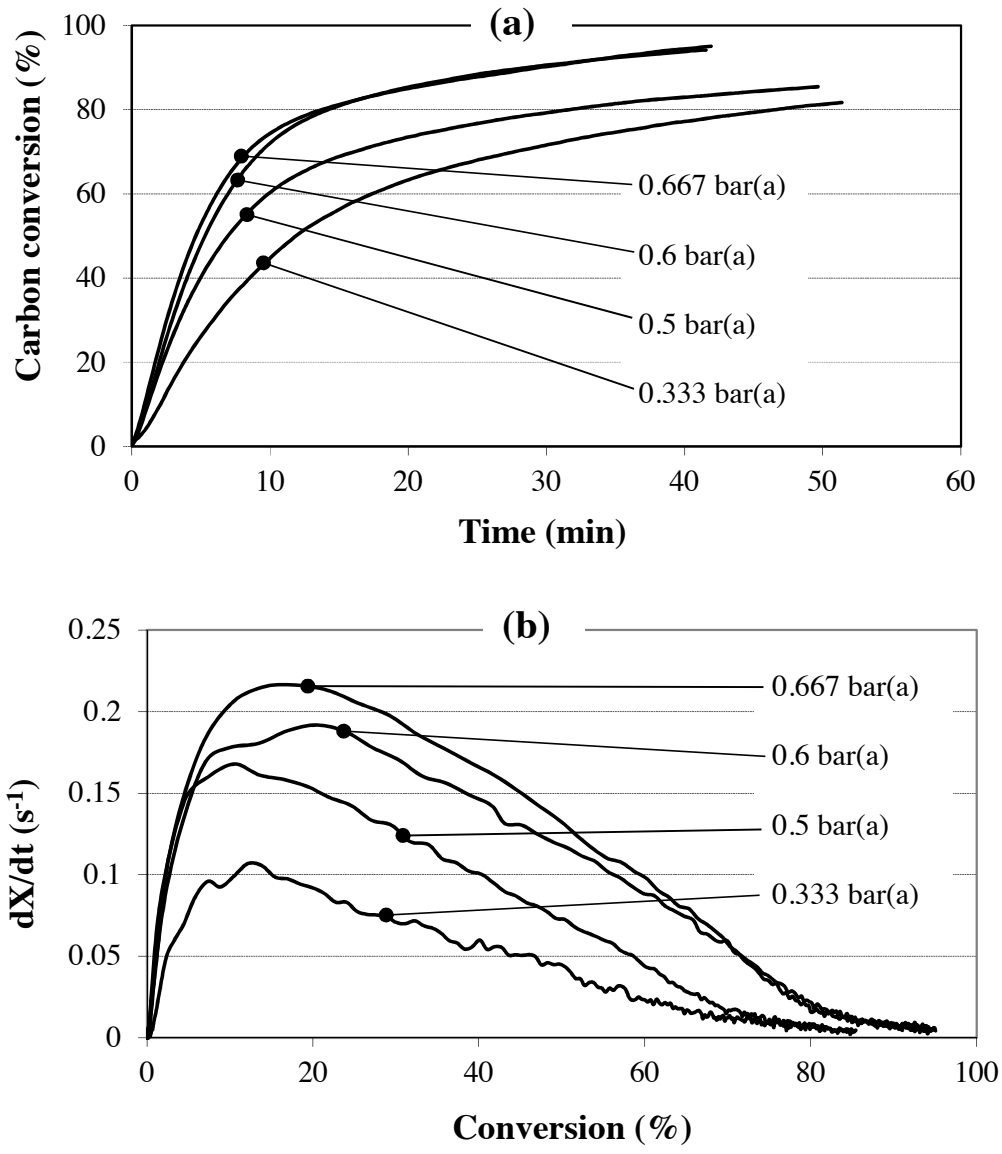

627

628 **Figure 4**

629

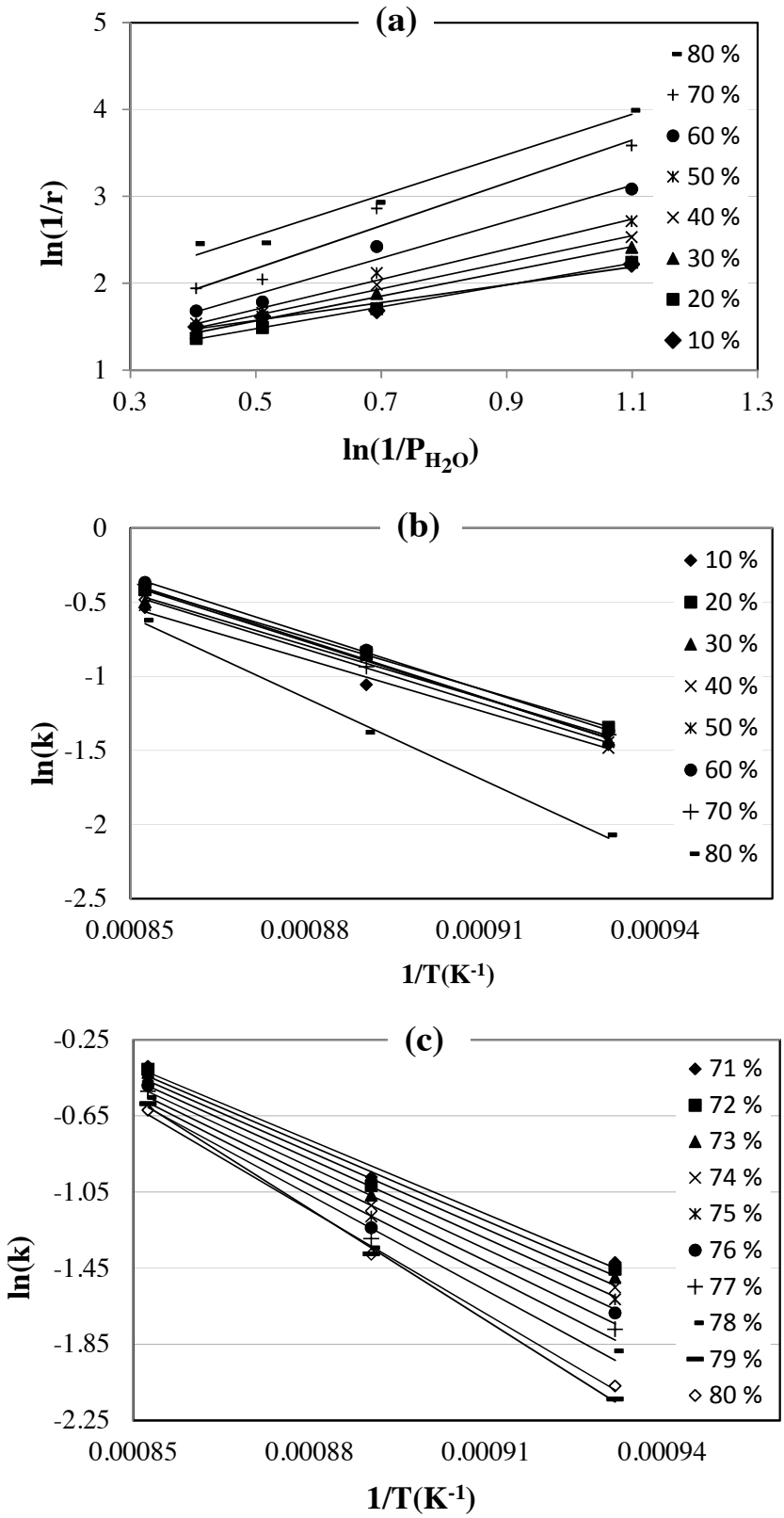
(a)
ln(1/r)
ln(1/P_H2O)
80 %
70 %
60 %
50 %
40 %
30 %
20 %
10 %
(b)
ln(k)
1/T(K-1)
10 %
20 %
30 %
40 %
50 %
60 %
70 %
80 %
(c)
ln(k)
1/T(K-1)
71 %
72 %
73 %
74 %
75 %
76 %
77 %
78 %
79 %
80 %

Figure 5

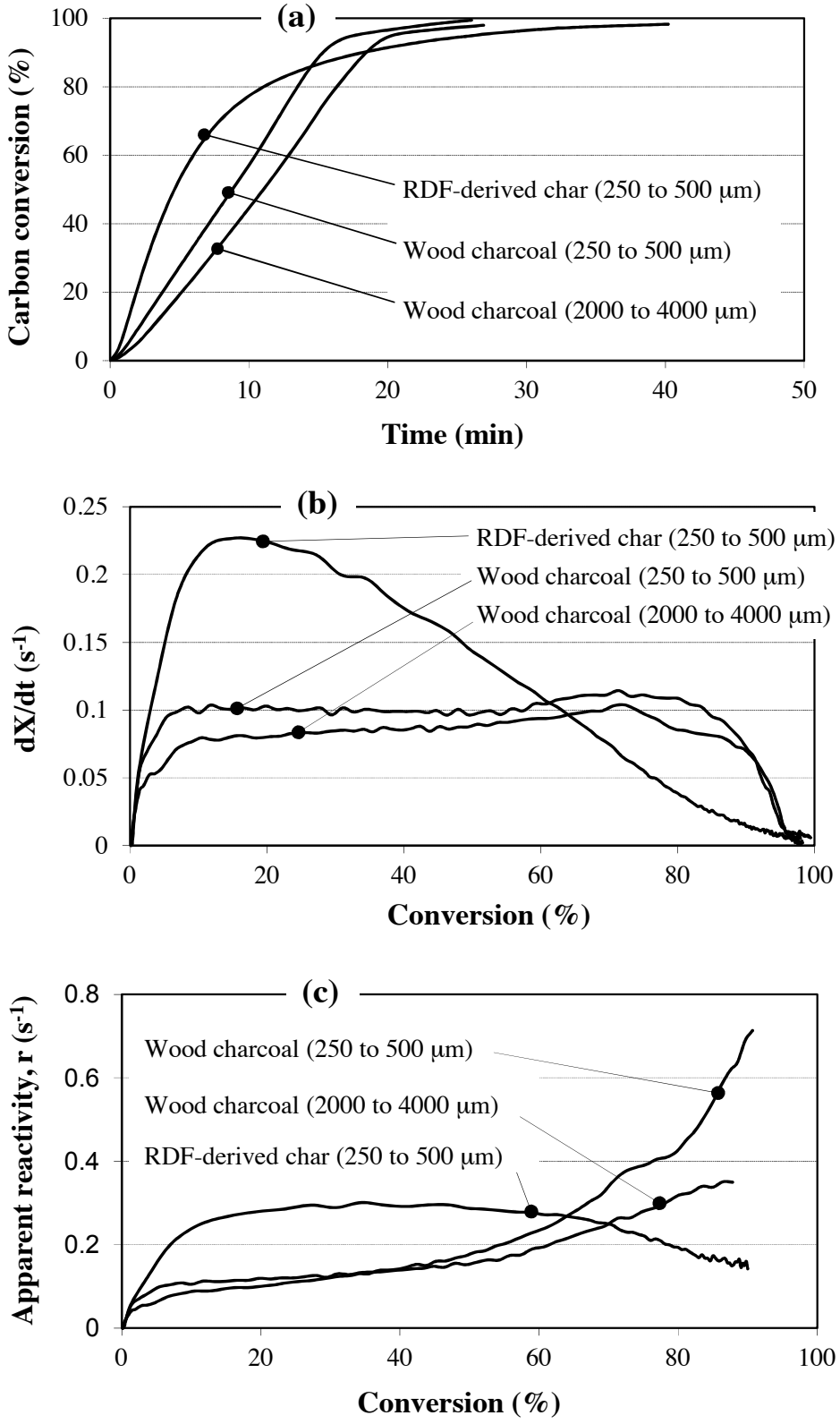

632

633 **Figure 6**

Table 1. Values of *k* and *n* at various reaction temperatures (Shrinking-Core Model).

Carbon	**900 °C**		**850 °C**		**800 °C**	
conversion (%)	***k***	***n***	***k***	***n***	***k***	***n***
10	0.585	1.453	0.347	1.025	0.232	0.889
20	0.660	1.413	0.429	1.261	0.261	1.075
30	0.607	1.370	0.427	1.429	0.239	1.179
40	0.594	1.409	0.421	1.529	0.226	1.216
50	0.639	1.579	0.435	1.732	0.235	1.382
60	0.693	1.878	0.439	2.092	0.254	1.810
70	0.684	2.286	0.393	2.466	0.248	2.351
80	0.537	2.676	0.252	2.333	0.126	2.937

637 **Table 2.** Apparent activation energies and pre-exponential factors (Shrinking-Core
638 Model).

Carbon conversion (%)	**Arrhenius equation** $\ln(k) = \ln(A) - \frac{E}{R_g}\frac{1}{T}$	**Apparent activation energy, *E* (kJ mol^{-1})**	**Pre-exponential factor, *A* (bar^{-n} s^{-1})**
10	y=9.342 – 11620x	96.6	1.14 x 10^4
20	y=9.5596 – 11696x	97.2	1.42 x 10^4
30	y= 9.5651 – 11768x	97.8	1.43 x 10^4
40	y= 9.9045 – 12182x	101	2.00 x 10^4
50	y=10.323 – 12597x	105	3.04 x 10^4
60	y=10.42 – 12644x	105	3.35 x 10^4
70	y=10.471 – 12756x	106	3.53 x 10^4
71	y=10.612 – 12942x	108	4.06 x 10^4
72	y=10.806 – 13195x	110	4.93 x 10^4
73	y= 11.061 – 13522x	112	6.36 x 10^4
74	y= 11.379 – 13926x	116	8.75 x 10^4
75	y= 11.765 – 14412x	120	12.9 x 10^4
76	y=12.225 – 14987x	125	20.4 x 10^4
77	y=12.798 – 15695x	131	36.1 x 10^4
78	y= 13.651 – 16724x	139	84.8 x 10^4
79	y= 16.035 – 19516x	162	92.0 x 10^5
80	y= 14.889 – 18220x	152	29.3 x 10^5

639 Note: When the conversion was calculated, using the equations presented in this table,
640 the match was within ± 5% of the experimental data obtained.
641
642

643 **Table 3.** Apparent activation energies and pre-exponential factors (Uniform-Reaction
644 Model).

Carbon conversion (%)	**Arrhenius equation** $\ln(k) = \ln(A) - \frac{E}{R_g}\frac{1}{T}$	**Apparent activation energy, *E* (kJ mol^{-1})**	**Pre-exponential factor, *A* (bar^{-n} s^{-1})**
10	y=9.3771 – 11620x	96.6	1.18 x 10^4
20	y=9.6351 – 11697x	97.2	1.53 x 10^4
30	y= 9.684 – 11768x	97.8	1.61 x 10^4
40	y= 10.075 – 12182x	101	2.37 x 10^4
50	y=10.555 – 12598x	105	3.84 x 10^4
60	y=10.725 – 12644x	105	4.55 x 10^4
70	y=10.873 – 12756x	106	5.27 x 10^4
71	y=11.023 – 12941x	108	6.13 x 10^4
72	y=11.231 – 13195x	110	7.54 x 10^4
73	y= 11.498 – 13522x	112	9.85 x 10^4
74	y= 11.828 – 13926x	116	13.7 x 10^4
75	y= 12.227 – 14412x	120	20.4 x 10^4
76	y=12.7 – 14987x	125	32.8 x 10^4
77	y=13.228 – 15695x	131	59.0 x 10^4
78	y= 14.155 – 16723x	139	14.0 x 10^5
79	y= 16.525 – 19482x	162	15.0 x 10^6
80	y=15.426 – 18220x	152	50.1 x 10^5

645 Note: When the conversion was calculated, using the equations presented in this table,
646 the match was within ± 5% of the experimental data obtained.